Investigation of Alternative Fuels Using Experimental and Computational Chemistry

Simon Chen[1], Winnie Chan[1], Carmen Chen[2], Olivia Kusio[2], Si On Kim[3], Raafiul Hossain[4], Vincent Wu[5], Melanie Chow[6],

[1]Cornell University, Ithaca, NY 14853
[2]Princeton University, Princeton, NJ 08544
[3]Stuyvesant High School, 345 Chambers St New York, NY 10282
[4]Binghamton University, 4400 Vestal Pkwy E, Binghamton, NY 13902
[5]The Cooper Union, 30 Cooper Square New York, NY 10001
[6]The University of Chicago, 5801 S Ellis Avenue, Chicago, IL 60637
raafiulhossain@gmailcom

Abstract: The aim of this study was to compare and explore potential alternative fuels through the use of computer-aided simulation techniques and laboratory experiments. Environmental influence, efficiency, cost, and availability were also taken into account in order to find the best replacement for fossil fuels. Bond energy, semi-empirical and density functional theory calculations were compared to known experimental heats of combustion. The results showed that the RM1 E+RT method (Method 1) was the most accurate and precise for predicting heats of combustion. A decision matrix was used to tally up rankings of each method under several statistical measures, leaving RM1 E+RT with the lowest overall score, due to its consistently high ranking for each statistical method. The RM1 E+RT graphical comparison with given literature gross heat of combustion (GHC) data made it feasible to predict experimental heats of combustion through the use of a linear regression equation: y=0.95x-12.158, with x representing literature GHC values and y representing predicted GHC values. It had a coefficient of determination of 0.998, percent error of 0.0557%, standard deviation percent error of 0.0476%, average unsigned error of 257 kJ/mol and a standard deviation unsigned error of 164 kJ/mol. After analysis and investigation of select alternative fuels to determine the most practical one, it was decided that ethane and biodiesel were the strongest candidates due to their low toxicity and corrosivity.

[Simon Chen, Winnie Chan, Carmen Chen, Olivia Kusio, Si On Kim, Raafiul Hossain, Vincent Wu , Melanie Chow **Investigation of Alternative Fuels Using Experimental and Computational Chemistry.** *Nat Sci* 2018;16(1):110-122]. ISSN 1545-0740 (print); ISSN 2375-7167 (online). http://www.sciencepub.net/nature. 13. doi:10.7537/marsnsj160118.13.

Keywords: alternative fuel, experimental and computational chemistry

1. Introduction

As nonrenewable energy resources dwindle and industries are pressured to examine their impact on the environment, the demand for clean alternative fuels grows remarkably. Current fossil fuels, such as coal, oil, and natural gas, are detrimental to climate patterns, the environment, and population health. They cause harmful greenhouse gases which pollute the atmosphere [1]. To tackle these setbacks, many industries work tirelessly to find and test clean alternative fuels, especially those that release large amounts of usable energy during combustion. Complete combustion is defined as the oxidation of a substance after ignition, the products of which are carbon dioxide, water, and heat. Net heat combustion (NHC) assumes that water is in the vapor state in the products of the reaction. Gross heat of combustion (GHC), which will be examined in this study, accounts for the heat of condensation of water [2]. GHC was chosen to account for the fact that water is a liquid at standard state. Different computational theories were used to model literature data, so that they could serve as a predictive tool where data is unavailable. Enthalpies were calculated using the given bond dissociation energy values and the following relation.

$$\Delta H \approx \sum \Delta H_{\text{(bonds broken)}} - \sum \Delta H_{\text{(bonds formed)}}.$$

Bond dissociation energies are defined as amounts of energy needed to break bonds. Computational methods were also used to calculate enthalpy and energy in order to evaluate which computational method is most accurate with respect to the literature gross heats of combustion values [3].

The computational methods are from a program called Spartan '14 v1.1.8 GUI, which is a molecular modeling and simulation program that performs several types of calculations, such as molecular mechanics, semi-empirical and ab initio methods, that numerically solve the Schrödinger equation. Molecular mechanics only focuses on the structural properties of common compounds found in fuels. Conversely, an ab initio (quantum) method, DFT, was chosen as more rigorous and time-consuming method to see the relationship between accuracy and computational time required.

The semi-empirical methods used for this study were the Austin Model 1 (AM1), Recife Model 1

(RM1), Parameterized Model number 3 (PM3), and Parameterized Model number 6 (PM6) methods. AM1 takes parameters describing Gaussian functions centered at different positions to describe the potential of mean force, which gives the average force of all reaction coordinates [13]. PM3 uses different Gaussian basis sets, but does not necessarily outperform AM1 [14]. RM1 offers optimized parameters of AM1, and corrects the inaccurate approximations of the net charge of nitrogen present in PM3 [14]. PM6 builds on the reference data that PM3 uses by including a much more expansive set, including over 9,000 discrete species, thereby increasing accuracy [15]. The DFT method used was Becke, three-parameter, Lee-Yang-Parr (B3LYP), which uses functionals (functions that take input vectors and output a scalar quantity), to represent electron densities in order to compute the probability of an electron at a given position in time [16,17]. This probability is then used to determine the location of the electrons where they are most likely to be found.

On another note, businesses are turning toward newer, cost-effective and non-toxic fuels. One of these types of fuels that is on the verge of replacing diesel is biodiesel [18]. They offer a promising replacement to fossil-based diesel due to their similar properties. In other words, biodiesels can be replaced as fuel for an existing engine without any major adjustments to technology while offering up to 280% energy yield compared to petroleum diesel fuel [19,20,21]. There are several key differences between normal diesel and biodiesel. Diesel is a clear, yellow-brown combustible liquid. It is a crude form of oil that is more pollutive than gasoline [18]. Biofuels are environmentally friendly alternative energy sources that are created using bio-based products. Biodiesels produced from oils with a large number of saturated fatty esters produce have a high cetane number; cetane number is the percent by volume of cetane (hexadecane) in diesel fuels. The high cetane number of biodiesel compared to that of standard diesel allows for easier ignition and a quieter engine [20].

Biodiesels were created in the laboratory to explore the principles of alternative fuel synthesis and to obtain thermodynamic and physical property data that could be compared to simulation data. Biodiesel was chosen to be examined in this study over other fuels due to its favorable properties. It is 100% renewable and has significantly lower levels of harmful pollutants and global warming gases [21]. In fact, according to the United States Environmental Protection Agency, biodiesel is one of the few fuels to pass the agency's rigorous health and emission tests [18].

Biodiesel is a substance that is created by transesterification of oils or fats such as vegetable oil, nut oils, animal fats, and seed oils. Transesterification is a process by which a triglyceride, a glycerol connected to three fatty acids by ester bonds [22,23], is added to an alcohol and a catalyst, producing glycerol, an undesirable product, and fatty acid methyl esters (FAMEs) (Figure 1). In this particular case, methanol was used as the alcohol and KOH as the catalyst. Biodiesel is largely composed of the FAMEs produced through this process. In figure 1 below, R1, R2, and R3 represent long hydrocarbon chains, typically between 12 and 24 carbon atoms, which may contain double bonds (in the case of an unsaturated fat) or only single bonds (in the case of a saturated fat).

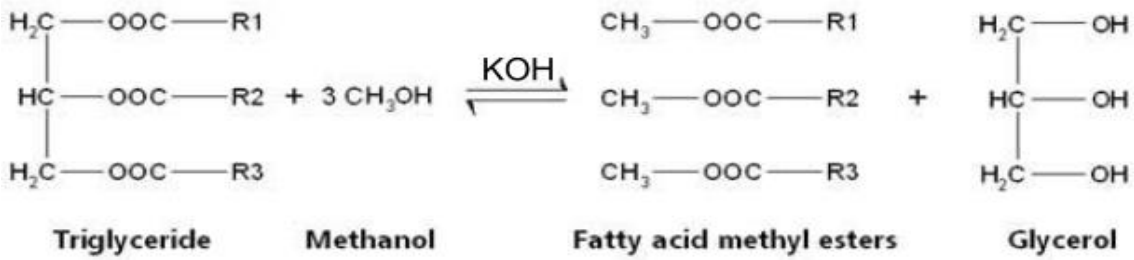

Figure 1 - Reaction of oil (triglyceride) with an alcohol (methanol) and a catalyst (KOH) to create biodiesel (FAMEs) and glycerol [18]

The biodiesels created in the laboratory were made with oils often found in a kitchen cabinet, such as olive oil, vegetable oil, and soybean oil. In addition, biodiesel utilizing used vegetable oil from Wendy's was also synthesized. The biodiesels were analyzed using gas chromatography-mass spectrometry (GC-MS). The GC-MS allows complex mixtures of chemicals in its components and offers both quantitative and qualitative analysis on the mixture to determine what compounds are in the mixture, as well as their relative amounts [24].

2. Computational Procedure

The most accurate method for finding the GHCs of compounds was determined by comparing the calculated values of each computational method with the literature values [3] for a set of 31 molecules. To most accurately determine the optimal method of predicting a fuel's heat of combustion, a test set consisting of a variety of sizes, isomers, and polarities was constructed such that there were a certain amount of alkanes, alkenes, alcohols, aldehydes, cis-trans isomers, aromatic compounds, carboxylic acids, cycloalkanes, amines, and sugars.

The first approach, using bond energies to compute GHCs, was utilized for each of the 31 molecules. Using the given bond energy table values [3] and the bond dissociation theory, GHC values were calculated for each molecule. In combustion, the bonds broken would be those of the reactants and bonds formed would be those of the products. Once initial GHCs were found, heats of vaporization and sublimation were subtracted from the GHC values from liquids and solids at standard state, respectively, since they are not in their gaseous forms at standard temperature. Also, the heat of The following are the generalized combustion reactions for CH, CHO, CHN and CHNO compounds [25].

Although using bond energies is a simple and straightforward procedure, it may not be accurate in correctly predicting the heats of combustion of potential fuels. For example, bond energies do not account for resonance (due to delocalized electrons) in aromatic compounds such as benzene. It also cannot distinguish between constitutional isomers (molecules with the same molecular formula but different structural formula) because they are comprised of the same bond types. Similarly, bond energies would predict identical heats of combustion for stereoisomers (molecules with the same structural formula but different three-dimensional shapes) for the same reason. Because of these limitations, more involved methods were employed.

These methods involved the use of Spartan, where a graphical user interface allowed the creation of a 3D model of a molecule from its atomic constituents. A geometry optimization was performed to calculate the lowest energy state. This was done by allowing the constituent bond lengths, bond angles and dihedral angles, the angles between planes involving three or more atoms, to vary. One possible complication was that different minimization energies may be computed from different 3D structures, which could affect the calculations. Different minimization energies may be computed if molecules are constructed in different ways. To combat this inherent variance, each molecule was modeled and minimized twice and the average calculated value was used. After minimization, calculations were performed for each semi-empirical method type, namely AM1, RM1, PM3 and PM6, with each molecule in its ground state configuration. Calculations were also performed for one DFT method using B3LYP as the parameter type. This method used a 6-31G* basis set, with each molecule in the ground state in a vacuum with no solvents. Based on these calculations and the concept that

$$\Delta H^\circ_{rxn} = \Sigma\, H^\circ f_{(products)} - \Sigma\, H^\circ f_{(reactants)},$$

heat of formation and internal energy values of each molecule, along with those of oxygen, carbon dioxide, and water (the main reactants and products in combustion), were used to calculate the GHCs in two different ways.

The first type of GHC calculation (Method 1) was based on the assumption that all of the compounds are ideal gases and rely on the internal energies of the molecules. Since the ideal gas law states that PV = nRT, the expression E+PV, which represents the enthalpy of the molecule in a system, can be also stated as E+nRT. Expressing this using intensive properties, the equation for heat of formation can be condensed into H=E+RT. Using the heats of formations calculated using E+RT, Hess's Law,

$$\Delta H^\circ_{rxn} = \Sigma\, \nu H^\circ f_{(products)} - \Sigma\, \nu H^\circ f_{(reactants)},$$

was used to find the GHCs. ν is the stoichiometric coefficient. This equation was used to calculate the GHCs of all 31 compounds at standard temperature, and again at each compound's ignition temperature, defined as the lowest temperature at which a compound spontaneously ignites in nature at standard pressure. Enthalpy at ignition temperature was calculated to get a sense of the compound's thermodynamic properties in actual combustion conditions, since most compounds do not combust spontaneously at standard temperature.

The second type of GHC calculation (Method 2) used Spartan-calculated enthalpy of formation values for all the compounds at standard state and at each compound's ignition temperature. Using these heat of formation values, GHCs were calculated in exactly the same way as in Method 1.

It should be noted that all calculations done by Spartan and bond energy values are assumed to be in gas-phase. In order to obtain the enthalpies at standard state, enthalpies associated with any necessary phase changes were taken into account due to the fact that some of the reactants and products may be liquids or solids at room temperature. Thus, heats of vaporization and sublimation were subtracted from the GHC values from liquids and solids at standard state, respectively, since they are not in their gaseous forms at standard temperature.

Because the heat of formation and energy values of water were assumed to be based on its gaseous form in Spartan, the reverse heat of vaporization for water,

44.016 kJ/mol, multiplied by the number of moles of water in the respective combustion reaction, was subtracted from each GHC value at standard state as well.

GHC values from both Method 1 and Method 2 were compared with the given literature values [3] to find the optimal method for determining GHCs of compounds. Once this method was found, it was used to compute the GHCs of the methyl esters found in the GC-MS data from the synthesized biodiesel. The following is the procedure for all lab-based chemistry that was conducted to synthesize and test various types of biodiesel and their respective GHCs.

3. Laboratory Procedure

The laboratory procedure was used to synthesize biodiesel and analyze properties such as density and dynamic viscosity. It was also used as a systematic way to measure the effectiveness of Spartan's various computational methods. The biodiesel procedure was based on a similar experiment developed by Loyola University Biodiesel Labs [26]. The oil samples used to create biodiesel were extra virgin olive oil (EVOO), soybean oil, hot dressing oil (mixture of soybean oil and mustard seed oil), expired olive oil (EVOO), extra-light virgin olive oil (ELVOO), and waste vegetable oil (WVO) from Wendy's. The WVO contained food particles from the frying process and needed to be filtered before transesterification [26]. The Loyola Lab procedure called for a 25 micron sock filter. Due to availability, a paper filter with 11 micron-sized pores was used. Since oil at room temperature is viscous and takes a long time to filter, a vacuum trap using a water aspirator was used to speed up the process. Once the large particles of the WVO were filtered out, the oil was heated to 70℃ in order to separate the water from the oil.

Loyola University Biodiesel Labs used 1 L of vegetable oil, 0.2 L of methanol, and 8.0 g of KOH [26]. Because of limited availability in oil, the measurements were scaled to maintain the same ratio of oil to methanol and KOH. Since KOH pellets were used, the amount of base used with each oil varied slightly. The process of transesterification required 50 mL of the oil, 10 mL of methanol, and approximately 0.4 grams of KOH.

WVO contains free fatty acids (FFAs) which are produced when water reacts with triglycerides. The FFAs react with base catalysts, producing soap while reducing the effective amount of catalyst [26]. To neutralize the FFAs, additional base catalyst was added. The amount of additional KOH needed was found by titrating a 0.1% KOH reagent solution with an analyte solution containing 20 mL of 2-propanol, three drops of phenolphthalein solution, and one mL of purified WVO. The total amount of KOH required for WVO was found using an equation that was derived by equating the ratio of the amount of oil used to 1 L of oil to the ratio of the amount of KOH needed to (8.0g KOH + T):

$$\frac{Amount\ of\ KOH\ (g)}{8.0\ g\ KOH + T\ (g)} = \frac{Amount\ of\ oil\ (L)}{1\ L}$$

T represents the total grams of reference solution needed to turn the analyte pink.

For each oil, the base catalyst was created by dissolving KOH pellets in methanol. The base catalyst and oil were mixed in a 50 mL round bottom flask and agitated in a sonicator for 60 minutes at 25℃. Due to a limited supply of sonicators, an alternate procedure was performed on the expired EVOO mixture. The mixture was moved to a separatory funnel and agitated by repeatedly inverting the funnel rightside up and upside down. The stopper was loosened after each shake to relieve pressure.

After agitation was complete, the mixtures were poured into separatory funnels and left to settle overnight. This process produced crude biodiesel because of contaminants such as methanol, basic salts, and glycerol [26]. In the separatory funnel, two layers formed, a biodiesel layer and a waste byproduct layer. The biodiesel was washed with approximately 1 mL of water to remove any remaining contaminants and then removed by opening the stopcock.

GC-MS samples were then created using hexane as a solvent. In order to obtain a concentration of around 100 ppm, five μ L of biodiesel were added to 50 mL of hexane in a volumetric flask so that the total volume was 50 mL. After mixing, each solution was placed in a GC-MS vial. Control solutions were also made by adding 0.1μ L of the oils used into approximately 1 mL of hexane. Samples were analyzed under specific conditions (Appendix B).

The density, viscosity, heat capacity, and heat of combustion of each biodiesel were measured. The density was found by measuring the volume of fuel in a beaker or graduated cylinder and weighing it to determine the mass so that the equation.

$$\rho = \frac{mass}{volume}$$

could be used to calculate density (ρ). To calculate viscosity, the formula.

$$\eta = \frac{2(ps-pf)g}{9v}r^2$$

was used, where r is the radius of the marble, v is the velocity, ρ_s is the density of the marble, ρ_f is the density of the biodiesel and g is the acceleration due to gravity [26]. A 16 mm diameter marble was dropped in a known volume of fluid that was placed in a graduated cylinder. As the radius of the marble approaches that of the graduated cylinder, the 'backflow' affects the velocity the marbles travels at through the fluid [27]. Two points along the graduated cylinder were marked and the time it took the marble

to travel between the points was recorded via stopwatch. The velocity of the marble was calculated by dividing the distance between the two points by the time it took for the marble to travel that distance. Three or four trials were conducted and the velocity was found by averaging the velocities from the trials. Heat capacity was found by recording the equilibrium temperature after combining 10 mL of hot fuel (between 60℃-70℃) with 10 mL of hexane. The biodiesels were heated to the approximate boiling point of hexane (65℃), so that no hexane would evaporate after mixing. Initially, the experiment was performed in such a way that the hexane was added to the hot fuel. Since the hexane was at a lower temperature and the thermocouple was in the hot fuel, the temperature of the mixture constantly decreased and it was not possible to get an accurate reading of the temperature after mixing. To try to remedy this inaccuracy, the temperature was recorded only after it stabilized temporarily and began to decrease slowly. Due to the high possibility of error, another approach was used for subsequent experiments. ELVOO was tested by adding the hot fuel to the hexane instead, with the thermocouple in the hexane. This way, the temperature increased and could be recorded at the highest point. In addition, the EVOO and expired EVOO samples were retested again using this procedure. Heat capacity was calculated by utilizing thermodynamics, as shown below.

$Q_{biodiesel} = - Q_{hexane}$

$Q_{biodiesel} = (ms\Delta T)_{biodiesel}$

$Q_{hexane} = (ms\Delta T)_{hexane}$

$S_{biodiesel} = - \frac{(ms\Delta T)hexane}{(m\Delta T)biodiesel}$

Q = heat (J), m = mass (g), s = specific heat (J/g℃), T = temperature (℃)

To determine heat of combustion, temperature changes in water were recorded as biodiesel was burned. In order to accomplish this, a tin can and a 100 mL round bottom flask were set up in a fume hood. A known quantity of biodiesel was placed inside the tin can and water inside the round bottom flask. After the masses of water and fuel were measured, the initial temperature of the water was recorded. A propane tank was used to light the fuel. Once the temperature of the water reached 50℃ for olive oil and soybean oil, the fuel was extinguished and the remaining fuel was weighed. However, for HDO, EVOO, and expired EVOO, the fuel was burned to completion to obtain a more accurate value on the mass of fuel used and the final temperature was recorded. In all cases, significant amounts of smoke were observed. In the case of WVO, the amount of smoke was severe and no burning took place. The equations $Q_{water} = (ms\Delta T)_{water}$ and $Q_{biodiesel} = -(\Delta H_C m)_{biodiesel}$ were used to calculate the GHC of biodiesel. The heat lost by the biodiesel was gained by the water, changing the temperature of the water, which means $(ms\Delta T)_{water} = -(\Delta H_C m)_{biodiesel}$. Solving for the GHC of biodiesel gives $\Delta H_c = \frac{-(ms\Delta T)}{mbiodiesel}$. It is important to note that this setup was not fully insulated, so heat loss was inevitable and contributed to some error in our experimentally calculated GHCs.

To calculate the relative molar amounts of each FAME, relative areas in the chromatograms on the GC-MS were used. A percent composition of each FAME by moles in the biodiesel was calculated by normalizing the relative amounts. The GHC of each biodiesel was found by scaling the contribution of the individual components by their relative amounts using the following equation:

$\Delta_c H_{biodiesel} = \Sigma (f_i * \Delta_c H_i)$

(Equation 1)

Where f is fractional abundance and i is a component.

The same additive method was used to calculate the apparent molar mass of the biodiesel:

$MM = \Sigma(f_i * MM_i)$

(Equation 2)

Where f is fractional abundance and i is a component.

By dividing the GHC (in kJ/mol) by the apparent molar mass, the GHC in kJ/g was computed. This was then substituted into the equation for the trendline to determine the corresponding experimental value. The experimental GHCs, from the laboratory were compared to these predicted GHCs, from Spartan. The predicted GHCs were found via the most accurate computational method found from the use of the trendline. The experimental and predicted GHCs were compared to accepted experimental heats of combustion from literature sources.

4. Results and Discussion

The different methods for calculating GHCs were compared by graphing the calculated values against the literature values to determine a linear regression for each method (Appendix A, figures A1-A5). Five statistical measurements were used to compare the results of the methods to the literature values: average percent error, standard deviation of percent error, average unsigned error, standard deviation of unsigned error, and coefficient of determination, or the R2 value.

Eleven computational methods were compared: five using Method 1, five using Method 2, and one using the bond energy values. The most accurate computational method was selected using a decision matrix in which all statistical measurements were assigned equal weight. Each calculation type was ranked from 1 to 11 in each statistical comparison.

The rankings were added across all statistical categories and final scores were tallied for each calculation type. The best calculation type was determined as the one with the lowest overall tally, meaning that it had the highest average rank (Table 1).

Using the sum of rankings to determine the best calculation type may be erroneous because the ranking system does not account for how close the measurements are to each other. An example of this lies in the comparison between the Bond Energy and PM6 Method 2 values in the average percent error category. The Bond Energy percent error is greater than that of the other methods combined but it is only one rank away from PM6 Method 2. In addition, this form of determining the best calculation type weighs all statistical methods equally and does not put any emphasis on any one statistical method. Furthermore, there were multiple difficulties in determining correct weights for each method. This difficulty is shown in the R2 values. Although it is the most important since the accuracy of the trendline is critical when determining the best computational method, all of the values were very close together. In fact, the range was only 0.00475. This suggests that using R2 values to compare methods would not be highly accurate.

To combat these complications, all statistical methods were treated equally.

Table 1 - Comparison of RM1 Methods 1 and 2 with literature values

Method	Rank	Average % Error	Rank	Standard Deviation % Error	Rank	Average Unsigned Error (kJ/mol)
Bond Energy	11	4.778	11	5.416	1	87.67
AM1 (M2)	3	0.08548	7	0.06619	6	383.1
PM3 (M2)	6	0.1199	9	0.09938	3	124.8
PM6 (M2)	10	0.3273	5	0.05692	11	654.6
RM1 (M2)	2	0.05674	10	0.1117	5	341.6
B3LYP (M2)	7	0.2227	1	0.04154	8	458.0
AM1 (M1)	5	0.09799	4	0.052718	7	386.2
PM3 (M1)	4	0.09224	8	0.090271	2	99.86
PM6 (M1)	9	0.2832	6	0.05881	10	609.3
RM1 (M1)	1	0.05572	2	0.04758	4	256.7
B3LYP (M1)	8	0.2527	3	0.0509	9	562.8

Method	Rank	Standard Deviation Unsigned Error (kJ/mol)	Rank	R Squared Value	Sum of Rankings
Bond Energy	1	83.52	7	0.9959	31
AM1 (M2)	5	257.8	9	0.9958	30
PM3 (M2)	3	154.1	6	0.9972	27
PM6 (M2)	9	495.4	3	0.9979	38
RM1 (M2)	11	527.6	8	0.9959	36
B3LYP (M2)	7	406.7	1	0.9986	24
AM1 (M1)	6	261.5	11	0.9938	33
PM3 (M1)	2	123.5	10	0.9946	26
PM6 (M1)	10	498.1	4	0.9978	39
RM1 (M1)	4	164.1	5	0.9976	16
B3LYP (M1)	8	473.5	2	0.9984	30

Consequently, RM1 Method 1 was determined to be the best method; it had the highest average rank out of all eleven computational methods. Additionally, its total tally of sixteen was eight lower than that of the second best method, B3LYP. This large difference is promising and reaffirms that it is the most accurate method (Figure 1). This was initially surprising because B3LYP was predicted to be the most accurate method, given that it is more complex algorithmically and takes into account more computations than the semi-empirical and bond energy methods. These results suggest that RM1 Method 1 is more optimized for the specific set of molecules tested in the study. However, the close R2 values of the models indicate that more testing on additional types of molecules and quantum mechanic models should be done to determine the accuracy to a greater degree.

The GHCs of the synthesized biodiesels were calculated using Equation 1 and Equation 2 as observed by the GC-MS chromatogram results. The final heat of combustion was found by substituting this result as the calculated value (y) in the RM1 Method 1 trendline equation, $y = .95x - 12.158$. These values

were then compared with the laboratory derived GHCs of the samples.

The FAME molecules were identified by analyzing the peaks of the GC-MS chromatograms of the biodiesels. The fragmentation patterns of the peaks were compared to literature data (Appendix C, figures C1-C5). Most of the peaks were determined to be methyl esters, which was expected. The other peaks found included peroxides, some alcohols, and different ketones. The peroxides formed as the oils aged and oxidized naturally over time. Ketones such as 2-hexanone are commonly found in vegetable oils [28]. Heptanone and pentanone were also found in the non-expired EVOO and the WVO in small amounts, but none of the ketones were found in the expired EVOO. These ketones may exist in the oils because microorganisms in the solution can oxidize free fatty acids and form ketones including heptanone and pentanone [28, 29]. This causes the purity of some of the biodiesels to lower. In the expired EVOO, however, it is possible that the hexanone evaporated out of the oil before it was converted to biodiesel because the hexanone is volatile, and the expired EVOO had a much longer shelf life than the non expired EVOO. Since it is a product of the transesterification reactions producing biodiesel, some amounts of octadecadienoic acid (Z,Z), methyl ester were found in each biodiesel. Surprisingly, a test run of only the hexanes showed a very high amount of octadecadienoic acid (Z,Z), methyl ester as well. This may be due to contamination of the container of hexanes. These increased levels of methyl ester increase the purity and heat of combustion of each biodiesel by showing a higher concentration of octadecadienoic acid (Z,Z), methyl ester than there may actually be.

During the biodiesel synthesis, it was discovered that there was residue from previous samples in the GC-MS after running blank samples, which may have affected original results.

In addition to standard state, the GHCs of the test compounds were found at ignition temperatures using RM1 Method 1. These values were compared to the values calculated at standard state with the same method but were not compared to literature data due to the lack of literature GHC values at ignition temperature. The GHCs were calculated at ignition temperature by running the Spartan calculations and changing the temperature of formation from 298.15 K to 772.15 K, which is the average ignition temperature of the biodiesels [30]. Since the GHC values were calculated with all reaction substituents in gaseous states, the heats of vaporization and the heats of sublimation for molecules that are non-gaseous at standard state were also accounted for [30]. These values were compared to the literature standard state values and the calculated standard state values from Spartan. The literature value for GHC of a biodiesel was found to be 41.2 kJ/g at standard state [31]. The GHCs calculated from Spartan were up to 5 kJ/g off from the literature value. The difference could have been because the Spartan model deemed to be most accurate for the test compounds does not accurately represent the molecules found in biodiesels.

It was observed that the majority of the biodiesel GHC values at ignition temperature were less than those at standard temperature. This is likely due to the fact that the ignition temperatures of biodiesels are higher than the boiling point of water. As a result, water-producing molecules do not condense. The exception to this is the expired EVOO. There are several possible explanations for this outlier. One possibility of the higher GHC at ignition temperature is that the expired EVOO's heat of vaporization is greater than the net heat of vaporizations of the water molecules. This means that more energy is needed to convert the reactants to gases than is released by the condensation of water at standard state. Alternatively, this could be due to the Spartan-calculated heats of formation being a function of temperature.

The Spartan-calculated GHC values for the fuels that successfully combusted were less than the literature value for every biodiesel [31]. One reason for this is that the Journal of Chemical Education study [31] on biodiesels used peanut oil which has a higher GHC than the fuels used in this study. Additionally, there were impurities from the biodiesel synthesis. These impurities affect the heat of combustion calculation from the RM1 Method 1 by reporting incorrect molar ratios. However, this result confirms that the experimental GHC values, not the calculated ones, are very far off.

The GHC of WVO-based biodiesel could not be measured experimentally, as it failed to continuously combust. It was observed that as the WVO biodiesel was heated at and above the average ignition temperature of biodiesel, the fuel smoked profusely and flames sporadically appeared on the surface. However, self-sustained combustion did not take place as the flames disappeared as soon as the biodiesel stopped being heated. A possible reason why fthe WVO biodiesel did not burn was that it was contaminated with water. It is likely that the WVO feedstock for the biodiesel had a higher concentration of water than the source oils for the other experimental biodiesels, since it came into contact with moist food and the surrounding air for extended periods of time. Water may have leached from the food or condensed from the air, contaminating the oil. There was an attempt to separate the water from the oil during the initial purifying process of the WVO, but no water separation was observed after heating the oil at 70℃

for over 15 minutes [26], signifying that water either failed to separate or was not present. Water was later intentionally added to the oil during the washing step, which followed the transesterification process. While a layer of water and water-soluble components was eluted out of the biodiesel after the wash step, it is possible that some water remained. Contamination by water lowers the heat of combustion and increases the smoking of a biodiesel [32]. These symptoms match prior observations of the WVO-based biodiesel combustion experiment, confirming that water prevented ignition.

Physical properties of biodiesel such as density, viscosity, specific heat capacity, and GHC values were determined through experiments. It was observed that the density values of the biodiesels were similar to the literature values from the Loyola Lab.

Heat loss was most likely because the procedure of calculating heat of combustion occurred under a fume hood, which produced a steady air flow, preventing the flame from the biodiesel from being concentrated under the flask with water. Moreover, the flask and its contents were heated by thermal conduction, which meant that the flame from the biodiesel had to not only heat the flask, but also the air around it [33]. This meant that there was some heat lost to the surroundings because the system wasn't insulated.

The biodiesel with the highest purity was discovered to be the EVOO, with 93.94% purity (Table 3). Releasing 38.60 kJ/g at standard temperature (Table 2), it ranked the highest in heat of combustion using Spartan computations. The more pure a biodiesel is, the more methyl esters it contains, allowing it to produce a greater amount of heat during combustion.

89.20% (Table 3) of the expired EVOO diesel was composed entirely of methyl esters, having a concentration significantly lower than the non-expired EVOO, as expected. The expired EVOO produced a greater amount of peroxides, due to its longer exposure to oxidation, lowering the purity. Additionally, it produced significantly less heat than the non expired EVOO, releasing 36.01 kJ/g (Table 2), according to Spartan calculations at standard temperature.

Table 2 - Biodiesel experimental properties and Spartan-calculated properties estimated to four significant figures

Biodiesel	GHC (kJ/g) (Experimental)	GHC (kJ/g) (Spartan Standard)	GHC (kJ/g) (Spartan Ignition)
Expired olive oil	-1.180	-36.01	-37.06
Olive oil	-1.805	-38.60	-36.72
Soybean	-1.895	-37.81	-35.96
Extra-light virgin olive oil	-1.173	-38.23	-36.35
Waste vegetable oil	N/A*	-38.53	-36.65
Waste vegetable oil rerun	N/A*	-35.24	-37.03
Hot dressing oil	0.8496	-38.20	-36.33

Table 3 - Biodiese l experimental properties

Biodiesel	Purity (%)	Density (kg/m3)	Viscosity (Pa*s)	Specific Heat Capacity(J/(g*°C))
Expired olive oil	89.21	875.0	1.861	0.8522
Olive oil	93.94	867.8	1.035	1.070
Soybean	93.33	864.2	2.555	0.9110
Extra-light virgin olive oil	92.81	865.2	1.432	1.335
Waste vegetable oil	87.43	887.7	3.77	0.9950
Hot dressing oil	89.08	879.0	1.136	0.6680
Literature Values	N/A	860 - 900	(34*10-4) - (51*10-4)	

For the WVO, Spartan computations calculated a heat of combustion of -38.53 kJ/g at standard temperature, which was similar to that of the EVOO. The soybean oil had the second highest purity, but did not have a relatively high heat of combustion, releasing only -37.81 kJ/g, purities. However, HDO released as much as 38.20 kJ/g, which was comparatively high (Table 2). All of the biodiesels had purities less than 95% (Table 3). In general, the impurities of the biodiesels may have caused experimental errors when determining heats of combustion, so it is possible these rankings vary slightly in reality.

The most significant factor when deciding whether an alternative fuel is favorable is the amount of heat it releases during combustion. However, it is critical to discuss environmental and economic factors in depth as well because they define the sustainability of the fuels and likeliness of introducing them as replacements for harmful fossil fuels. Ignition temperatures must also be examined because a lower ignition temperature allows for a lower kinetic threshold, which is the lowest temperature a fuel can

spontaneously ignite. Additionally, a low heat capacity of the fuel is favorable. The heat given off by a fuel can be measured by the equation, $Q = ms\Delta T$. Since s and ΔT are inversely proportional, when s decrease, ΔT increases, which signifies that less energy is required for the fuel to reach its ignition temperature.

Another important characteristic of efficient and sustainable fuel is cost. An unaffordable fuel is useless for industrial applications even if it releases a large amount of heat and is environmentally promising. Many alternative fuels, such as naphthalene, have to be imported from countries such as China because they are not easily found in the United States [34]. Effective transportation methods for the fuels are also critical. Corrosivity is a crucial factor to consider because fluids are often transported in metal drums or pipes, and fluids with high corrosivity can weaken the durability of the metal containers. Kinematic viscosity was also considered and is defined as the amount of resistance in a liquid measured by η/ρ (viscosity divided by density). The lower the viscosity, the less resistance/internal friction the fuel will have, and the closer it would be to a laminar flow, a model condition where the fuel travels the smoothest [35].

Toxicity is also a critical measurement because environmental and health factors must to satisfied in order for the fuel to be feasible. Toxicity can be measured in two different ways: Lethal Dose 50 (LD50) and Lethal Concentration 50 (LC50). LD50 is the dosage of a drug that can kill fifty percent of the tested population when consumed. LC50 has a similar definition, except that the drug is inhaled rather than consumed. LD50 & LC50 both use two variables to measure toxicity: concentration (in parts per million) and time (in hours). Since these two variables are exponentially related, it was determined that the molecule that can have the highest concentration in the body for the longest period of time was the safest.

Table 4 summarizes the preferable characteristics of an ideal alternative fuel.

Table 4 - Characteristics of an ideal fuel

Ideal characteristics of Alternative Fuels:
Heat Capacity: Low
Heat of Combustion: High
Cost: Low
Toxicity: No
Ignition temp: Low
Corrosive: No
Kinematic viscosity: Low
Availability: Extremely Available

When deciding on which fuel is applicable, it is paramount to consider all of the characteristics mentioned above. There are many fuels that have great advantages in certain ways, yet possess issues in other ways. As seen in Table 5, fuels, such as naphthalene, that have a high heat of combustion and a low heat capacity pose dangerous health risks that eliminate them from being potential alternative fuels. According to the International Agency for Research on Cancer (IARC) [36], it is highly carcinogenic, proving naphthalene to be unfeasible as an alternative fuel [34]. Gasoline also has a high heat of combustion and is widely accessible, many vehicles use it as its primary fuel source. But like naphthalene, gasoline, according to the IARC, is highly carcinogenic. Another fuel that has a low heat capacity and high heat of combustion but is practically unsuitable due to its toxicity is ammonia (Table 6), which differs from methanol because it is synthesized via hydrogen from natural gases and nitrogen from the atmosphere while methanol comes from natural gas [37]. It is also very expensive to synthesize because the plants used to create the biomethanol in the fermentation process often cost a lot of money [37].

Table 5 - Top 5 rankings of researched alternative fuels

Ranking	Lowest Heat Capacity (J/(mol * K))	Highest Heat of Combustion (kJ/g)	Lowest Cost (per kg)	Lowest Toxicity (based on effect on human body)	HighestSustainability	Lowest Kinematic Viscosity (m2/s)	LowestCorrosivity
1	Methane(34.92)	Ammonia(-74.41)	Methanol($0.12)	Biomethanol	Ethane	Ammonia(3.00E-7)	Ethane
2	Ammonia(35.06)	Methane(-55.49)	Ammonia($0.14)	Methanol	Bioethanol	Methanol(7.02E-7)	Butanol
3	Methanol(52.29)	Ethane(-51.88)	Ethane($0.19)	(Bio)ethanol	Biodiesel	Ethane(7.55E-7)	Naphthalene
4	Ethane(52.8)	Naphthalene(-40.18)	Ethanol($0.20)	Biodiesel	Ammonia	Naphthalene(9.69E-7)	Bioethanol
5	Ethanol(78.28)	Biodiesel(-39.8)	Acetic Acid($0.26)	Acetic Acid	Methane	Acetic Acid(1.08E-6)	Acetic Acid

For fuels like bioethanol, properties such as toxicity, heat of combustion and heat capacity are not issues of concern. However, transportation and storage feasibility become major problems. Because bioethanol creation technologies are not currently available, it is difficult for many third world countries to maintain their production and must rely on importation for fuel. In addition, bioethanol has a high corrosivity. Thus, while bioethanol may fill some of the criteria for an ideal alternative fuel, it is not practical. One fuel that is a strong candidate for an alternative fuel where transportation is not a critical

issue is ethane. According to Table 5, ethane is ranked fourth in lowest heat capacity, third in highest heat of combustion, first in highest sustainability and second in most atmospheric abundance [38]. It also costs $0.19 per kilogram, which is the third cheapest fuel in our data set, and experts claim that those prices could drop in the near future due to the abundance of ethane [39]. Due to relatively cheap prices, companies could set up ethane-cracking stations, which would be an efficient way of getting ethane, around the world [40,41]. Since it naturally degrades in water and air, it is almost harmless to the environment. Ultimately, because ethane satisfies many of the ideal characteristics of a fuel and does not display any large disadvantages for usage, it is a very strong candidate for an ideal fuel. Biodiesel is also a good candidate. It is a reliable alternative to petroleum diesel and has many benefits. Biodiesel is very sustainable because it can be manufactured from many common resources, such as vegetable oil, animal fats, and used restaurant oil [42]. Furthermore, it is a renewable fuel and, because of the versatile resources it can emerge from, can be easily produced domestically, greatly reducing America's dependence on foreign oil imports [42]. In addition, biodiesel is less toxic than petroleum diesel and, if used widely, can significantly reduce exposure to harmful fumes [42]. Other noteworthy characteristics of biodiesel are its low vapor pressure and flammability. These properties can be useful when, for example, biodiesel is handled in a confined space such as a mine. On the other hand, they can be hindrances when used with engines starting at cold temperatures [43].

Table 6 -Toxicities of researched fuels

Molecule	Time (hr)	Concentration(ppm)
Acetic Acid	5620	1
Ammonia	1.159	1
Biodiesel	7640	4
Bioethanol	20000	10
Biomethanol	8600	72
Butanol	8000	4
Ethane	658	4
Ethanol	20000	10
Methane	0.326	2
Methanol	64000	4
Naphthalene	170	4

5. Conclusion

After much computation and lab work, significant conclusions can be drawn about which alternative fuels release the largest amount of energy, while being cost-effective, readily available and sustainable in the near future. Here are key results of this study:

1. Computational methods via Spartan have shown that RM1 Method 1 is the most accurate for calculations on molecules. This method was determined to be the best by comparing the eleven methods used and ranking each method according to statistical measurements such as average percent error, standard deviation, average unsigned error, and coefficient of determination. Each method was given a total tally based on the sum of all its rankings and RM1 Method 1 had the lowest tally (16). The coefficient of determination statistic was not weighted more than the others because all R2 values were within an extremely short margin of one another.

2. Spartan calculations and experimental GHC values of the synthesized biodiesels were substantially different, due to heat loss and biodiesel impurities. Heat loss occurred as the biodiesels were burned under a fume hood; the flame not only heated the flask filled with water, but also its surroundings. All biodiesels were under 95% in purity, which may account for the low GHCs during experimentation.

3. Typically, the biodiesels that contained more methyl esters (greater purity) resulted in greater heats of combustion, while those with greater amounts of peroxides (less pure) resulted in lower heats of combustion. EVOO, with a 93.94% purity, had the greatest GHC (-38.60 kJ/g) in Spartan calculations, as opposed to the expired EVOO's lower GHC (-36.01 kJ/g) with a lower purity (89.20%.) However, the experimentally-derived GHC value for EVOO was the highest, most likely due to experimental errors. ELVOO also had a high purity (92.81%), but a low experimental GHC value (1.173 kJ/g.) The greater GHC value from Spartan calculations (-38.53 kJ/g) further suggested experimental errors.

4. Significant properties of a favorable alternative fuel included a high heat of combustion value, minor environmental impact, low heat capacity, low ignition temperature, low kinematic viscosity, low toxicity, no corrosivity, and low cost. Ethane ranks relatively high in every category; it is the most sustainable alternative fuel, is abundant on earth, and has a fair heat capacity and heat of combustion. Biodiesel is another promising fuel as it is completely renewable and extremely versatile in production. It also yields energy up to 280% of what petroleum diesel produces [42]. Ethane and biodiesel are potential substitutes for petroleum-based fuels.

5. After considering health hazards, cost, and sustainability, many possible fuels, such as ammonia, methane and naphthalene, can be dismissed. The dangerous properties of these fuels, namely their corrosiveness and carcinogenic effects, outweigh the benefits of their high heats of combustion and low heat capacities.

These conclusions have also left many key questions for future studies including how other kinds of bio-based fuels may be better alternative fuel sources and that there may in fact be a more precise computational method that the ones discussed in the study. Hartree-Fock (HF) and Moller Plesset (MP) are some of the other methods Spartan uses and can definitely be tested in future studies.

It is difficult to compare calculated values from Spartan with experimental data. Spartan creates molecules from atomic constituents unlike how moles are naturally formed. Spartan determined enthalpy and energy values at different local minimum energy points, which could vary depending on how the molecule was first constructed via the Spartan graphical user interface. This introduced an inherent flaw to the data, although this was somewhat combatted by taking the average of two of the same calculations. Only values at standard state were compared since values at ignition temperatures are not readily known due to experimental error and the relatively high ignition temperatures of some of the larger molecular weight compounds.

In addition, the method in which the most accurate (with respect to literature values) Spartan method was determined was somewhat flawed due to the fact that not all statistical measurements were actually equivalent in weight. The coefficients of determination were all very close, so R2 was not a good predictor of the best method. On top of that, the effects of percent error could be due to averages of much larger and much smaller values, giving an inaccurate assessment of the actual error in some of the methods. Nonetheless, with the tally approach used in this study, RM1 Method 1 was the clear winner by more than eight tallies. It is important to note also that although the ab initio method, DFT B3LYP, was the most mathematically demanding and complex method, using functionals to determine probabilities of electron positions, it was not the most accurate or precise method according to literature values at standard state. For semi-empirical methods, Spartan calculations were completed in a matter of minutes for both the test compounds and the compounds observed in biodiesel. Conversely, for large molecules such as those found in biodiesel, DFT B3LYP took up to hours for calculations to be completed.

One shortcoming in the fuel comparison aspect of this study was that the biomethanol and bioethanol literature GHCs were very hard to find due to the variety of ways in which these fuels are synthesized at multiple labs from previous research papers. This made combustion energy comparisons unpredictable with these fuels as compared to other potential alternative fuels.

Gratitude:

This research paper would not be possible without generosity and supervision of Prof. Savizky at The Cooper Union New York.

Abbreviations:

Abbreviation	Meaning
AM1	Austin Model 1 (Semi-Empirical)
B3LYP	Becke Three-parameter, Lee-Yang-Parr Functional (Density Functional Theory)
FA	Fatty Acid
FAME	Fatty Acid Methyl Ester
GC-MS	Gas Chromatography Mass Spectrometry
GHC	Gross Heat of Combustion
HDO	Hot Dressing Oil (Soybean Oil and Mustard Seed Oil)
LC50	Lethal Concentration 50
LD50	Lethal Dosage 50
NHC	Net Heat of Combustion
PM3	Parameterized Model Number 3 (Semi-Empirical)
PM6	Parameterized Model Number 6 (Semi-Empirical)
RM1	Recife Model 1 (Semi-Empirical)
WVO	Waste Vegetable Oil (Wendy's Vegetable Oil)

References

1. Union of Concerned Scientists. http://www.ucsusa.org/clean_energy/our-energy-choices/coal-and-other-fossil-fue ls/the-hidden-cost-of-fossil.html#.V6NOQUYwi70 (accessed Aug. 9, 2016).
2. Rojey, A.; Jeffret, C. et al. Natural gas: production, processing, transport; Editions Technip: Paris, 1997, 3.1.8, 108.
3. Atkins, P. W.; Paula, J. D. Physical chemistry, 7th edition.W H Freeman, 2007, 1076-1077.
4. Molecular Mechanics http://www.sdsc.edu/~kimb/molmech.html (accessed Aug 8, 2016).
5. UC Santa Barbara. http://people.chem.ucsb.edu/kahn/kalju/chem226/public/semiemp_intro.html (accessed Aug 9, 2016).
6. Chivian, D. Ab Initio Methods. Wiley-Liss, Inc., Hoboken, New Jersey, United States, 2003.
7. Georgia Tech. http://vergil.chemistry.gatech.edu/notes/hf-intro/node7.html (accessed Aug 9, 2016).
8. Cui, P. Møller-Plesset Many Body Perturbation Theory. North Dakota State University June 10,

2015. https://www.ndsu.edu/pubweb/kilinagroup/_files/MP2.pdf (accessed Aug 9, 2016).
9. Sherrill, C.D. Introduction to Electron Correlation. School of Chemistry and Biochemistry Georgia Institute of Technology. http://vergil.chemistry.gatech.edu/courses/chem6485/pdf/intro-e-correlation.pdf (accessed Aug 9, 2016).
10. Huzinaga, S.; Cantu A. A. Theory of Separability of Many-Electron Systems J.Chem. Phys. 1971, 55, 5543.
11. Hanninen,V. Introduction to Computational Chemistry. Laboratory of Physical Chemistry. Sept 20, 2012. http://www.helsinki.fi/kemia/fysikaalinen/opetus/jlk/luennot/Lecture4.pdf (accessed Aug 9, 2016).
12. Clugston, M. J.; Flemming, R. Advanced chemistry; Oxford University Press: Oxford, 2000, 5.6., 68-69.
13. Mills, K. Potentials of Mean Force as a Starting Point for Understanding Biomolecular Interactions, Ph.D. Thesis, University of Michigan, Michigan, United States, 2010, 1.1.2, 2-3.
14. Rocha, G. RM1: a reparameterization of AM1 for H, C, N, O, P, S, F, Cl, Br, and I. Thesis, Departamento de Química Fundamental, Recife PE, Brazil, 2003, 1.
15. Stewart, J. J. P. Optimization of parameters for semiempirical methods V: Modification of NDDO approximations and application to 70 elements. Journal of Molecular Modeling [Online] 2007 http://www.ncbi.nlm.nih.gov/pmc/articles/PMC2039871/ (accessed Aug 9, 2016).
16. Reimers, J. Computational Methods for Large Systems: Electronic Structure Approaches for Biotechnology and Nanotechnology, John Wiley & Sons, Inc., Hoboken, New Jersey, 2011.
17. Maitra, N.T. Perspective: Fundamental aspects of time-dependent density functional theory J. Chem. Phys. 2016, 144, 220901.
18. Diesel Fuel; OSHA IMIS No. D150 [Online]; United States Department of Labor: Washington, DC, Aug 10, 2006. www.osha.gov/dts/chemicalsampling/data/CH_234655.html (accessed Aug 9, 2016).
19. Pacific Biodiesel. http://www.biodiesel.com/biodiesel/benefits/ (accessed Aug. 9,2016).
20. Teoh, Y. H.; Masjuki, H. H.; Kalam, M. A.s Comparative assessment of performance, emissions and combustion characteristics of gasoline/diesel and gasoline/biodiesel in a dual-fuel engine, H. G. RSC Adv. 2015, 5(88), 71608.
21. American Lung Association ®, Clean Fuels: Biodiesel, Clean Air Choice, 2014.
22. Albers, H.; Guilfoyle, B.; Thelen, M.; Walker, C. Project Proposal and Feasibility Study, 2014.
23. Patil, P. Biodiesel Production from Waste Cooking Oil Using Sulfuric Acid and Microwave Irradiation Processes. New Mexico State University, Las Cruces, USA, 2012.
24. University of Bristol. http://www.bris.ac.uk/nerclsmsf/techniques/gcms.html (accessed Aug 9, 2016).
25. Domalski, Eugene S. Selected Values of Heats of Combustion and Heats of Formation of Organic Compounds Containing the Elements C, H, N, O, P, and S. Journal of Physical and Chemical Reference Data, 221 1972.
26. Waickman, Z. Biodiesel Labs; Loyola University of Chicago Institute of Environmental Sustainability Biodiesel Program: Chicago, IL 2013.
27. Singh, A. V.; Sharma, L.; Ghupta-Bhaya, P. Studies on Falling Ball Viscometries Departments of Chemistry, Material Science Programme, Indian Institute of Technology Kanpur, India, 2012.
28. Aparicio-Ruiz, R.; Harwood, J. Ed. Handbook of Olive Oil: Analysis and Properties; Springer Science & Business Media, 2013.
29. 2-Hexanone; CAS No. 591-78-6 [Online]; Agency for Toxic Substances and Disease Registry: Atlanta, GA, Sept. 1995. http://www.atsdr.cdc.gov/toxfaqs/tfacts44.pdf (accessed Aug. 9, 2016).
30. Somandepalli, V.; Kelly, S.; Davis, S. Hot Surface Ignition of Ethanol-blended Fuels and Biodiesel; doi:10.4271/2008-01-0402; SAE International: Detroit, Michigan, 2008.
31. Akers, S. M.; Conkle, J. L.; Thomas, S. N.; Rider, K. B. Determination of the Heat of Combustion of Biodiesel Using Bomb Calorimetry J Chem. Educ. [Online] 2006, http://pubs.acs.org/doi/abs/10.1021/ed083p260 (accessed Aug 9, 2016).
32. Atadashi, I.M.; Aroua, M.K.; Abdul Aziz, A.R.; Sulaiman, N.M.N, The effects of water on biodiesel production and refining technologies: A review. Renewable and Sustainable Energy Reviews [Online] 2012, 3456-3470. http://dx.doi.org/10.1016/j.rser.2012.03.004 (accessed Aug 10, 2016).
33. Gonzalez, C. What's the Difference Between Conduction, Convection, and Radiation? Machine Design [Online], 2015. http://machinedesign.com/whats-difference-between/what-s-difference-between-c_onduction-

convection-and-radiation (accessed Aug 9, 2016).
34. The Dollar Business. https://www.thedollarbusiness.com/news/imports-of-naphthalene-in-both-its-form s-crude-naphthalene/46846 (accessed Aug 9, 2016).
35. Georgia State University. http://hyperphysics.phy-astr.gsu.edu/hbase/pfric.html (accessed Aug 10, 2016).
36. https://monographs.iarc.fr/ENG/Monographs/vol82/mono82.pdf.
37. Nakagawa, H.; Harada, T.; Ichinose, T.; Matsumoto, S.; Takeno, K.; Sakai, M. Food and Fertilizer Technology Center [Online] 2015 http://www.fftc.agnet.org/library.php?func=view & style= & type_id=4 & id=201107 25161023 & print=1 (accessed Aug 9, 2016).
38. Simpson, IJ. Long-term decline of global atmospheric ethane concentrations and implications for methane, Nature [Online] Aug 23, 2012 http://www.ncbi.nlm.nih.gov/pubmed (accessed Aug 9, 2016).
39. Butler, N. Ethane the Next challenge for the Energy. Financial Times, [Online], Jan 18, 2015. http://blogs.ft.com/nick-butler/2015/01/18/ethane-the-next-challenge-for-the-ener gy-market/ (accessed Aug 9, 2016).
40. Detrow, S. The Ethane Cracker's Pollution Potential. State Impact, [Online], March 26, 2012. https://stateimpact.npr.org/pennsylvania/2012/03/26/the-ethane-crackers-pollution-potential/ (accessed Aug 9, 2017).
41. Ethane; CAS No. 74-84-0 [Online]; Exxon Mobil Chemical, Aug. 2013. https://www.exxonmobilchemical.com/Chem-English/Files/Resources/ethane-pro duct-safety-summary.pdf (accessed Aug. 9, 2016).
42. Crimson Renewable Energy, L.P. http://www.crimsonrenewable.com/specs.php (accessed Aug 9, 2017).
43. Oilgae. http://www.oilgae.com/energy/sou/ae/re/be/bd/char/char.html (accessed Aug 9, 2016).
44. Hexadecanoic acid, methyl ester http://webbook.nist.gov/cgi/cbook.cgi?ID=C112390 & Mask=200#Mass-Spec (accessed Aug 9, 2016).
45. 7-Octadecenoic acid, methyl ester http://webbook.nist.gov/cgi/inchi?id=c57396982 (accessed Aug 9, 2017).
46. Nonanoic acid, methyl ester http://webbook.nist.gov/cgi/cbook.cgi?id=c1731846 (accessed Aug 9, 2016).
47. 9,12-Octadecadienoic acid (Z,Z)-, methyl ester http://webbook.nist.gov/cgi/cbook.cgi?ID=C112630 & Mask=200#Mass-Spec (accessed Aug 9, 2016).
48. 2-Pentanone,5-hydroxy http://webbook.nist.gov/cgi/cbook.cgi?ID=C1071734 & Mask=200#Mass-Spec (accessed Aug 9, 2016).
49. Pentadecanoic acid, methyl ester http://webbook.nist.gov/cgi/cbook.cgi?ID=C7132641 & Mask=200#Mass-Spec (accessed Aug 9, 2018).
50. Tert -butyl hydroperoxide http://sdbs.db.aist.go.jp/sdbs/cgi-bin/direct_frame_top.cgi (accessed Aug 9, 2016).
51. 2-heptanone, 3-methyl http://webbook.nist.gov/cgi/inchi?ID=C2371199 & Mask=200#Mass-Spec (accessed Aug 9, 2016).
52. 2-hexanone http://webbook.nist.gov/cgi/cbook.cgi?ID=C591786 & Mask=1A8F#Mass-Spec (accessed Aug 9, 2016).
53. 9-octadecenoic acid http://webbook.nist.gov/cgi/cbook.cgi?ID=C112629 & Mask=200#Mass-Spec (accessed Aug 9, 2016).
54. 6-octadecenoic acid http://sdbs.db.aist.go.jp/sdbs/cgi-bin/direct_frame_top.cgi (accessed Aug 10, 2016).
55. Pentadecanoic acid http://webbook.nist.gov/cgi/cbook.cgi?Name=pentadecanoic+acid & Units=SI & c MS=on#Mass-Spec (accessed Aug 10, 2016).
56. 9,15-octadecadienoic acid http://sdbs.db.aist.go.jp/sdbs/cgi-bin/direct_frame_top.cgi (accessed Aug 10, 2016).
57. 8-octadecenoic acid.
58. Trans-13-Octadecenoic acid, methyl ester http://webbook.nist.gov/cgi/inchi?ID=U333613 & Mask=200 (accessed Aug 9, 2017).
59. 11-Hexadecen-1-ol http://webbook.nist.gov/cgi/cbook.cgi?ID=C56683546 & Mask=200 (accessed Aug 9, 2017).

9/29/2018